A Journal of the Gesellschaft Deutscher Chemiker

Angewandte International Edition Chemie

GDCh

www.angewandte.org

Accepted Article

Title: Interweavable Metalloporphyrin-based Fibers for Indirect Electrocatalysis

Authors: Xiaoman Yao, Gang Liu, Yingying Huang, Caier Huang, Xuanxu Chen, Zhe Xuan, Mingjin Shi, Yiwen Yang, Xianqiang Huang, Yifa Chen, and Ya-Qian Lan

To be cited as: *Angew. Chem. Int. Ed.* **2024**, e202417439

Link to VoR: https://doi.org/10.1002/anie.202417439

WILEY VCH

10.1002/anie.202417439

WILEY-VCH

RESEARCH ARTICLE

Interweavable Metalloporphyrin-based Fibers for Indirect Electrocatalysis

Xiaoman Yao[a]‡, Gang Liu[b]‡, Yingying Huang[a]‡, Caier Huang[a], Xuanxu Chen[a], Zhe Xuan[a], Mingjin Shi[a], Yiwen Yang[a], Xianqiang Huang[b], Yifa Chen[a]*, and Ya-Qian Lan[a]*

[a] X. Y., Y. H., C. H., X. C., Z. X., M. S., Y. Y., Prof. Y. C., and Prof. Y. -Q. L
Guangdong Provincial Key Laboratory of Carbon Dioxide Resource Utilization, School of Chemistry
South China Normal University
Guangzhou, 510006, P. R. China
E-mail: chyf927821@163.com; E-mail: yqlan@m.scnu.edu.cn

[b] G. L. and X. H.
Shandong Provincial Key Laboratory of Chemical Energy Storage and Novel Cell Technology, School of Chemistry & Chemical Engineering
Liaocheng University
Liaocheng, Shandong, 252059, P. R. China.

‡ Xiaoman Yao, Gang Liu and Yingying Huang contributed equally to this work.

Supporting information for this article is given via a link at the end of the document.

Abstract: The applications of indirect electrocatalysis toward potential industrial processes are drastically limited by the utilization or processing forms of electrocatalysts. The remaining challenges of electrocatalysts like the recycling in homogeneous systems or pulverization in heterogeneous systems call for advanced processing forms to meet the desired requirements. Here, we report a series of metalloporphyrin-based polymer fibers (M-PF, M = Ni, Cu and Zn) through a rigid-flexible polymerization strategy based on rigid metalloporphyrin and flexible thiourea units that can be applied as heterogenous redox-mediators in indirect electrocatalysis. These functional fibers with high strength and flexibility exhibit interweavable and designable functions that can be processed into different fiber-forms like knotted, two-spiral, three-ply, five-ply fibers or even interweaved networks. Interestingly, they can be readily applied in S-S bond cleaving/cyclization reaction or extended oxidative self-coupling reaction of thiols with high efficiency. Remarkably, it enables the scale-up production (1.25 g in a batch-experiment) under laboratory conditions.

Introduction

Organic electrosynthesis is regard as a sustainable and promising technique for the efficient production of value-added products and can be basically divided into direct electrolysis and indirect electrolysis systems.[1] Among them, direct electrolysis involves the direct contact between electrocatalyst and electrode, while the indirect one is achieved through the electrocatalysis interaction in the electrolyte.[2] Interestingly, employing a redox mediator, indirect electrolysis provides various advantages when compared with direct one, in which the reaction efficiency is improved with reduced energy consumption by avoiding electrode passivation and reducing the overpotential of electron transfer.[3] At the same time, the atomic economy will also be improved by avoiding the use of chemical oxidants or reductants.[4] Nevertheless, there are still some challenges for the commonly reported redox mediators, for example, the recycling problems for most of homogeneous redox mediators[5] or pulverization problems for some heterogeneous redox mediators in powder forms.[6] Specifically, the heterogeneous redox mediators in powder forms would be transformed into tiny powders during the indirect electrocatalysis, which would block the device, cause unstable reaction activity or even safety issues like explosion, largely dampening their potentials in practical applications. Thus, it would be much necessary to design and fabricate redox mediators with advanced processing forms for the potentially practical applications of indirect electrocatalysis.[7]

Polymer fiber, originating from nature and mastered by humans, is a kind of slender material with unique features including a high length-to-diameter ratio, large surface area, ease of storage/transportation, and enabled secondary processing or weaving and so on.[8] Up to date, it has been widely applied in a broad range of fields like textiles, construction, healthcare, automotive or aerospace, etc.[9] Polymer fiber will also be an ideal candidate as redox mediators in indirect electrocatalysis if unique electrocatalytic functions can be integrated, which might achieve processable, recyclable and efficient heterogeneous indirect electrocatalysis system with much potential for real catalysis scenarios like flowing bed catalysis or industrial-scale production.[10] Besides, properties like flexibility or rigidity of polymer fiber are also important as they are closely related to the durability during the electrocatalysis process, while the balance between them remains a giant challenge owing to the difficulty in multi-functional material design.[11] In this regard, we propose to assemble rigid metalloporphyrin and flexible thiourea units to produce a kind of robust redox mediators for heterogeneous indirect electrocatalysis system based on the following considerations: 1) metalloporphyrin unit as a rigid component with metal sites make fibers to be potential indirect electrocatalyst; 2) thiourea unit as a flexible component might endow the fiber with high flexibility that enables to be processed into advanced electrocatalyst forms; 3) the integration of them will create a powerful fiber based redox mediator with the combination of both rigidity and flexibility, abundant active sites, and high processability to meet the stringent requirements of heterogeneous indirect electrocatalysis. Nevertheless, it is still

10.1002/anie.202417439

hard in designing such interesting fiber based electrocatalysts and rare examples about polymer fiber based heterogeneous redox mediators have been reported as far as we know.

Here, we have successfully fabricated a series of mechanically robust metalloporphyrin-based polymer fibers (M = Ni, Cu and Zn) with indirect electrocatalytic properties through a rigid-flexible polymerization strategy based on rigid metalloporphyrin and flexible thiourea units (Scheme 1). These functional fibers with high strength and flexibility exhibit excellent interweavable and designable functions that can be readily processed into different fiber forms like knotted, two-spiral, three-ply, five-ply fibers or even interweaved networks. Interestingly, they can be readily applied in S-S bond cleaving/cyclization reaction or extended oxidative self-coupling reaction of thiols with high efficiency. Meanwhile, they can be easily recycled and enable to be fitted into gram-scale indirect electrocatalysis, which might provide new insights for designing novel electrocatalysts with advanced processing forms.

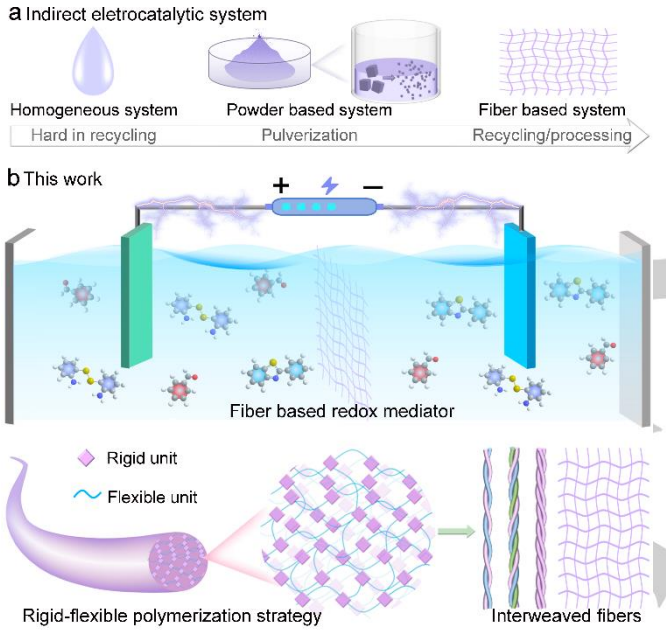

Scheme 1. The schematic illustration of the advantages of fiber based redox mediator in indirect electrocatalysis. (a) The challenges faced by traditional indirect electrocatalytic systems and the advantages of fiber based system. (b) The advantages of fiber based redox mediator in indirect electrocatalysis.

Results and Discussion

Structure and characterization.

M-PF (M = Ni, Cu and Zn) were synthesized by a thiourea-forming condensation reaction through a facile heating polymerization process with the assembly of metalloporphyrin (M-TAPP, M = Ni, Cu and Zn) and 1,4-diisocyanate (PDI) in capillary tubes with different diameters (Figure 1a, detail see Experimental Section). The fiber diameter and length can be controlled by simply using varied pipelines with pre-determined length and inner diameter. The initially formed polymer fibers were released from pipeline in a wet and adhesive state, and then dried in air at room temperature overnight. For instance, the Ni-PF with a length of about ~17 cm was obtained through these processes (Figure 1b).

To verify the composition of M-PF (M = Ni, Cu and Zn), Fourier-transform infrared spectroscopy (FTIR) tests were conducted to detect the characteristic groups. Taking Ni-PF as an example, the C=N stretching vibration band at 1615 cm^{-1} ascribing to Ni-TAPP maintains almost unchanged in Ni-PF in FTIR measurements, implying the retained Ni-porphyrin unit in Ni-PF.[12] Besides, the disappeared peak at 2000-2200 cm^{-1} of the obvious characteristic stretching band in the isothiocyanate group of PDI and two peaks of N-C=S (1650 cm^{-1}) and N-H (3200 cm^{-1}) belonging to thiourea group emerge obviously, confirming the formation of thiourea bond in Ni-PF.[13] In addition, the successful condensation of M-TAPP (M = Cu and Zn) and PDI has also been proved by their FTIR spectra (Figure 1c and S1). In addition, the PXRD patterns exhibit the amorphous characteristics of M-PF (M = Ni, Cu and Zn), which indicates the almost complete condensation reaction between metalloporphyrin and PDI in achieving a kind of homogenous polymer state (Figure 1d and S2).

Moreover, X-ray photoelectron spectroscopy (XPS) measurements were conducted on M-PF (M = Ni, Cu and Zn) to detect the elements. The results present that five main peaks are ascribed to Ni 2p, S 2p, N 2p and C 1s, respectively. In the S 2p region, two kinds of peaks with binding energy of 164.1 eV and 164.6 eV can be attributed to the characteristic peaks of sulfur in thiourea groups (Figure 1e).[14] Besides, the satellite peak at 400.4 eV is ascribed to the porphyrin unit, while the peaks at 398.7 eV and 399.6 eV belong to the pyrrolic N and amine groups in N 1s spectrum, respectively. Furthermore, two deconvolution peaks located at 855.1 eV and 872.4 eV are observed, attributed to Ni 2p3/2 and Ni 2p1/2 of Ni 2p spectra, respectively, which certifies the bivalent state of Ni.[15] In addition, the bivalent states of Cu and Zn for Cu-PF and Zn-PF have also been verified by their relative XPS spectra (Figure S3-6).

Scanning electron microscope (SEM) and energy-dispersive X-ray spectroscopy (EDS) element mapping tests are identified to characterize the morphology of M-PF (M = Ni, Cu and Zn). For example, the diameter of Ni-PF is detected to be ~180 μm and keeps uniform along the fiber. The surface of the fiber is smooth and uniform without any noticeable structural defects. Moreover, EDS mapping images present that Ni, S and N are evenly distributed in Ni-PF, validating the uniformity of the polymerization reaction (Figure 1f). Similarly, SEM and EDS mapping tests of Cu-PF and Zn-PF have also been carried out. The results display that the characteristic elements are uniformly distributed on Cu-PF and Zn-PF (Figure S7 and S8).

10.1002/anie.202417439

RESEARCH ARTICLE

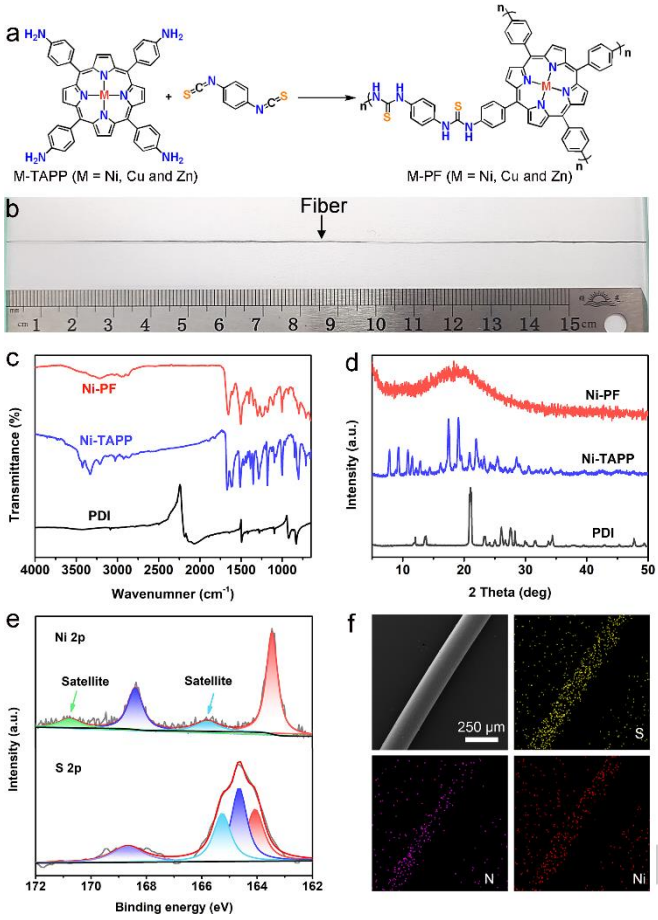

Figure 1. Characterization of Ni-PF. (a) The formation of M-PF (M = Ni, Cu and Zn). (b) The photograph image of a single fiber of Ni-PF. (c) FT-IR spectra of PDI, Ni-TAPP and Ni-PF. (d) PXRD pattern of PDI, Ni-TAPP and Ni-PF. (e) XPS spectra of Ni-PF. (f) SEM and EDS mapping images of Ni-PF.

The mechanical properties of M-PF (M = Ni, Cu and Zn) were systematically evaluated regarding ultimate tensile strength and Young's modulus using tensile tests. The tensile stress and strain of Ni-PF, Cu-PF, Zn-PF and TAPP-PF reach at 80.08 MPa (29.33%), 85.24 MPa (50.00%), 63.44 MPa (24.60%) and 67.04 MPa (17.49%), respectively, implying the superior mechanical properties of the as-prepared fibers (Figure 2a). In contrast to TAPP-PF, Ni-PF and Cu-PF exhibit higher tensile stress while Zn-PF has close property to TAPP-PF. Meanwhile, all of them have better strain properties than TAPP-PF, validating the impact of metalloporphyrin unit on the enhancement of mechanical performance. Specifically, there are obvious yield platforms in stress-strain curves, which indicates their good plasticity and flexibility as well as the vital role of rigid-flexible polymerization strategy in conferring fibers with both rigidity and flexibility. Furthermore, Young's modulus values of 1.91 GPa, 2.40 GPa, 1.53 GPa and 2.27 GPa are achieved by Ni-PF, Cu-PF, Zn-PF and TAPP-PF, which are superior to many common polymers like polyvinylidene fluoride, polytetrafluoroethylene, polyethylene and so on (Figure 2b). The mechanical strength of these fibers would set a fundamental basis for further processing and indirect electrocatalysis applications.

In addition to these basic characteristics, the robust fibers can be further shaped or readily processed into desired fiber-based devices. The shaping and processing of fibers are based on the wet and adhesive state before drying, during which the pre-obtained fibers can be shaped with molds or processed by further treatments. For instance, after curving the pre-obtained Ni-PF into coil along a glass rod, a kind of Ni-PF coil can be produced after drying process (Figure 2c). In addition, after knotting treatment of the pre-obtained Ni-PF, a knotted fiber with tight and steady state has been achieved (Figure 2d). Based on this pre-obtained Ni-PF in wet and adhesive state, it can be further interweaved. For example, if two pre-obtained Ni-PF are twisted together, a kind of tightly connected two-spiral fiber is readily obtained (Figure 2e). Similarly, Ni-PF in three-ply and five-ply yarn forms can be fabricated through similar protocols (Figure 2f and g). With this concept in mind, it can also be extended to fibers with different components. An interesting two-spiral fiber has been processed in a twisted form that can tightly integrate Ni-PF and Cu-PF together (Figure 2h). Besides, it can also be fitted into three-ply fiber with the integration of Ni-PF, Cu-PF and Zn-PF (Figure 2i). The shaping or processing properties of these fibers hold much promise in further interweaving treatment to achieve multi-component fibers with advanced forms to meet diverse application requirements.

10.1002/anie.202417439

RESEARCH ARTICLE

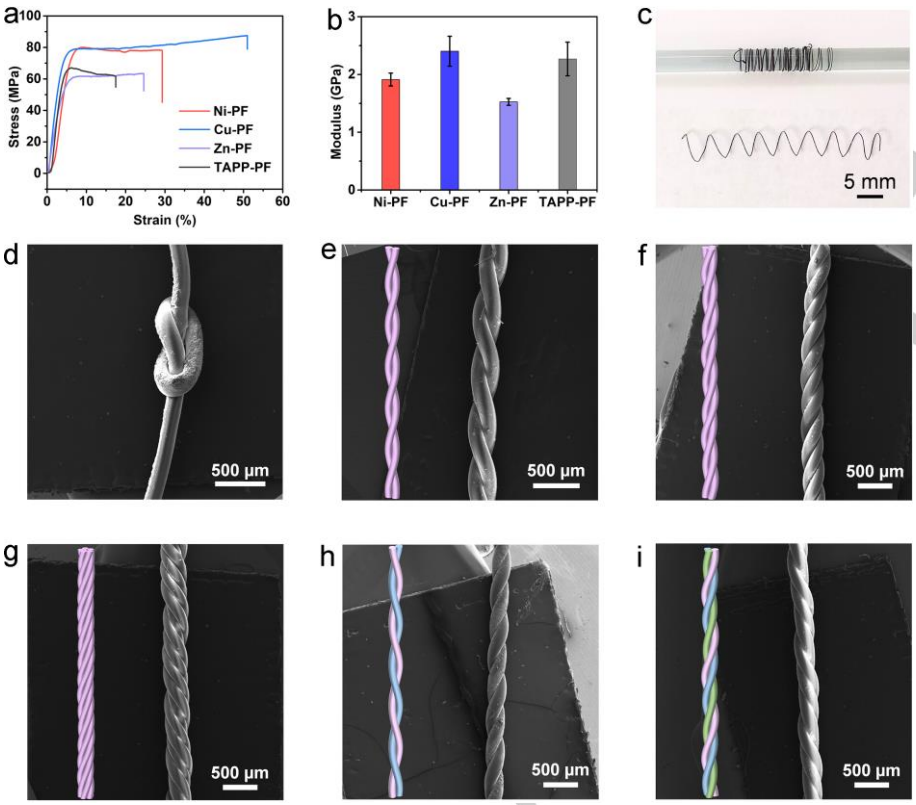

Figure 2. Morphology and flexibility of M-PF (M = Ni, Cu and Zn). (a) Tensile strength of M-PF and TAPP-PF. (b) Modulus of M-PF and TAPP-PF. (c) The photographs of Ni-PF coiled in bundle around the glass rod and coiled individually. (d) SEM image of the knotted Ni-PF. (e) SEM image of two spiral Ni-PF. (f) SEM image of three-ply Ni-PF. (g) SEM image of five-ply Ni-PF. (h) SEM image of two spiral polymer fibers of Ni-PF and Cu-PF. (i) SEM image of three-ply polymer fibers of Ni-PF, Cu-PF and Zn-PF.

Electrocatalytic property of M-PF (M = Ni, Cu and Zn)

2-Arybenzothiazole and its derivatives have excellent physiological and pharmacological value as precursors of various drugs like antitumor, antibacterial, antiproliferative or anti-inflammatory drugs for resisting tumor, lung, colon, breast cancer or Alzheimer's disease.[16] Based on the above superior properties of M-PF (M = Ni, Cu and Zn), we further set out to explore their possibility as redox mediators for green synthesis of 2-Arybenzothiazole and its derivatives in indirect electrocatalysis.[17]

In the indirect electrocatalysis tests, the counter and reference electrodes were Pt foil and Ag/Ag^+ electrode while the carbon plate was the working electrode. In order to evaluate the electrocatalytic activity of M-PF (M = Ni, Cu and Zn), the cyclic voltammetry (CV) measurements with a scan rate of 50 mV s^{-1} were performed. They were carried out with methanol containing tetrabutylammonium tetrafluoroborate (n-Bu_4NBF_4) as the electrolyte. After adding M-PF (M = Ni, Cu and Zn) as electrocatalysts, the oxidation potentials are obviously lower than that of TAPP-PF (Figure S9a), which reflects the rapid catalytic response of electrocatalysts to electrochemical oxidation. Besides, the resulting oxidation potential response of Ni-PF is lowest in CV curves, showing that Ni-PF is the optimal one in activating the reactants to make the reduction easier (Figure S9a). Therefore, we select Ni-PF as the desired electrocatalyst to investigate its indirect electrocatalysis property. Simultaneously, the onset potential of Ni-PF was determined via linear sweep voltammetry (LSV) and it found that the potential of electron transfer steps started at 0.3 V (vs. Ag/Ag^+), which shows the fast electron transfer ability of the Ni-PF under low potential (Figure S9b).

To further investigate the optimum reaction conditions of S-S bond cleaving/cyclization reaction in indirect electrocatalysis, the catalyst amount, constant current, solvent, and electrolyte have been investigated. The reaction based on 2,2'-disulfanediyldianiline (**1a**) and benzaldehyde (**1b**) in the generation of 2-arybenzothiazole (**1c**) was selected as a model reaction for Ni-PF (Table 1). Initially, the electrocatalytic property was studied at different time intervals (Figure 3a). The reaction yield of **1c** by Ni-PF gradually increases along with the reaction time and reaches to 93% at 8 h. After that, it remains almost intact with a longer reaction time, implying 8 h to be the optimal reaction time. In contrast, the **1c** yields of Cu-PF and Zn-PF gradually increase along with the reaction time from 2-10 h, and only 35% and 18% yields can be achieved after 8 h, respectively (Figure 3a and b). In sharp contrast, TAPP-PF has negligible catalytic effect (Figure 3b). In addition, different solvents including acetonitrile (MeCN), dichloromethane (DCM), ethanol (EtOH) and MeOH were optimized. The results show that MeOH exhibits the highest electrochemical performance with a yield of 93%, which is superior to MeCN (86%), DCM (80%), and EtOH (87%) (Figure S10). Besides, tetrabutylammonium bromide (TBAB), tri-n-butylamine (TBEA) and lithium perchlorate ($LiClO_4$) were further evaluated as electrolytes. In detail, TBAB (62%), TBEA (65%) and $LiClO_4$ (72%) all show much lower performances than that of n-Bu4NBF4 (93%), verifying that n-Bu_4NBF_4 is the most appropriate electrolyte (Figure S11). In addition, we further explored the

10.1002/anie.202417439

influence of catalyst amount on the performance (Figure 3c). The results present that the yields enhance with the increased dosage of Ni-PF less than 30 mg, and remain almost constant with more amount of Ni-PF (Figure 3c). Additionally, the constant current was also optimized and 7 mA was determined to be the optimal one. Besides, it shows high electrochemical stability of the reaction under different potentials and currents (Figure 3d and S12). Therefore, Ni-PF exhibits superior electrochemical activity under the optimized conditions.

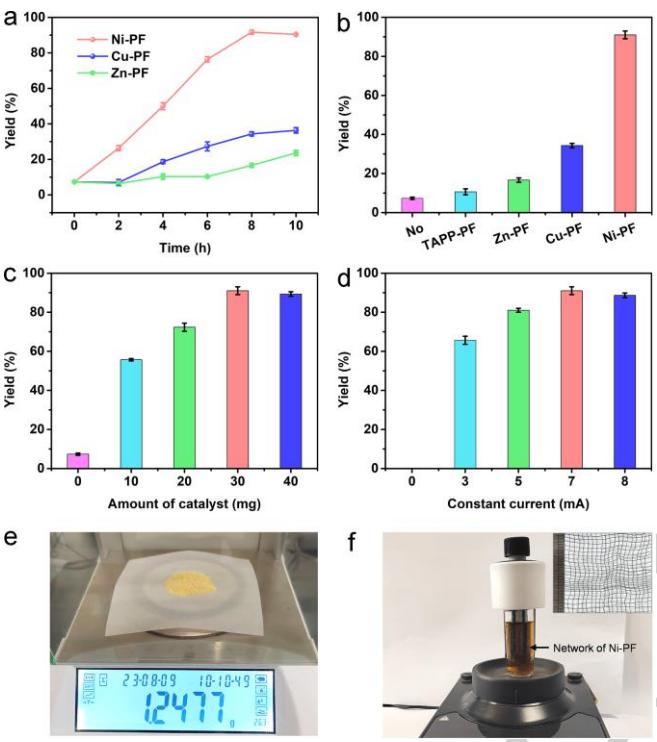

Figure 3. Electrocatalytic performance of M-PF (M = Ni, Cu and Zn). (a) Reaction kinetic analyses of Ni-PF, Cu-PF and Zn-PF. (b) The effect of different catalysts. (c) The effect of Ni-PF mass on the performance. (d) The effect of various current of Ni-PF. (e) Product photograph image of the gram-scale experiment. (f) Fiber-based network of Ni-PF interweaved on gauze.

Based on the superior electrochemical activity of Ni-PF, the scope of the S-S bond cleaving/cyclization reaction catalyzed by Ni-PF under optimal conditions was investigated. The substituted benzaldehyde b is used to react with **1a** to give product **c** (Table 1). When **1b** and **1a** are selected as the substrates, an excellent yield of **1c** (93%) is achieved by Ni-PF. When applying benzaldehydes b with electron-withdrawing groups (i.e. -Br and -F) in reaction with **1a**, the corresponding reactions give the expected products **2c** and **3c** with yields of 88% and 85%, respectively, which are both lower than that of **1c**. To further study the position impact of electron-withdrawing group (-Br) on the yield of products, p-bromobenzaldehyde, m-bromobenzaldehyde and o-bromobenzaldehyde were used to react with **1a**. Interestingly, the yields of **3c**, **4c** and **5c** are detected to be 85%, 80% and 70%, respectively, verifying the important group-position effect of electron-withdrawing group on the performance in indirect electrocatalysis. In addition, electron-donating groups like $-CH_3$ and $-OCH_3$ have also been studied and the desired products (**6c**, **7c** and **8c**) are obtained in varied yields (Table 1).

In addition, with the optimized conditions of the S-S bond cleaving/cyclization reaction system, we further extend the compatibilities of this methodology to the self-coupling reaction of S-H bonds based on a variety of substituted thiophenols to construct symmetric disulfides (Table 2). Initially, thioalcohols such as thiophenol was evaluated and it could generate product **1e** with a yield of 99%. Substituted thiophenols bearing electron-withdrawing groups (-Cl and $-NO_2$) and electron-donating groups at para-($-CH_3$, $-OCH_3$, and $-NH_2$) underwent the reactions, producing the desired products **2e**-**7e** in excellent yield (85-99%). Specifically, comparing with the 93% yield of **5e**, the slightly lower yield of **6e** might be because of the influence of the closer electron-donating group. Bicyclic ring derivatives including 2-mercaptobenzathiazole **8d** were also converted into 2,2-dibenzothiazole disulfide **8e** in 74% yield due to the steric effect (Table 2).

Long-term stability and recyclability of the catalyst were investigated based on Ni-PF with the optimal property. Taking the production of **1c** as a model reaction, the electrochemical curve of long term indirect electrocatalysis presents almost no fluctuation, which suggests high electrochemical stability of the reaction (Figure S13). In recycling experiments, before being reused in the successive reactions, the fiber based electrocatalyst could be easily separated after each cycle. After five cycles, Ni-PF only has a slight decrease in the yield (Figure S14). Furthermore, the PXRD and FTIR tests were complemented to verify the structure stability, in which PXRD patterns and FTIR spectra of M-PF (M = Ni, Cu and Zn) almost overlap and no obvious changes were detected (Figure S15-17). Furthermore, since the recycling ability of electrocatalyst plays a crucial role in indirect electrocatalysis, we have also prepared a kind of Ni-PF with integrated Fe_3O_4 nanoparticles that can be easily attracted and gathered by a magnet in solvents for easy recycling (Figure S18). Besides, the industrial applicability of this indirect electrocatalytic methodology was evaluated based on the optimal test conditions. We performed the scale-up synthesis of 2-arybenzothiazole under optimal conditions. Remarkably, ~1.25 g **1c** could be obtained in a batch experiment under laboratory conditions, which holds much promise in scale-up production for potential industrial applications (Figure 3e, detail see Supporting Information). In addition, an interesting fiber-based network interweaved on gauze was stuck in the reactor of indirect electrocatalysis system. Interestingly, Ni-PF based network could achieve a remained high yield of 95% in the production of **1c**. These results prove that Ni-PF enables to be applied in the processable, recyclable and efficient heterogeneous indirect electrocatalysis system, which would hold much potential for real catalysis scenarios like flowing bed catalysis or industrial-scale production (Figure 3f).

Table 1. Substrate scope of benzothiazoles catalyzed by Ni-PF.[a,b]

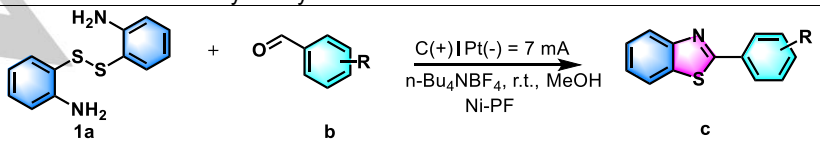

10.1002/anie.202417439

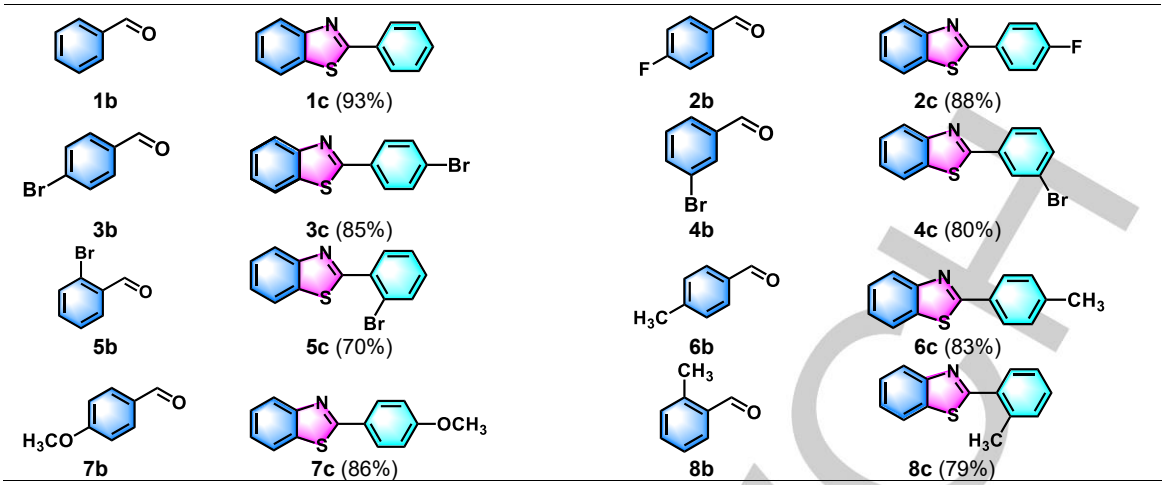

[a]Reaction conditions: carbon plate (53 mm * 8 mm * 1.5 mm) as anode, platinum plate (53 mm * 8 mm * 1.5 mm) as cathode, constant current (7 mA), 1a (0.2 mmol), b (0.4 mmol), Ni-PF (30 mg), n-Bu_4NBF_4 (0.25 mmol), CH_3OH (6 mL), r.t., 8 h. [b]Isolated yield..

Based on the above results and reported references,[18] we propose that the condensation reaction of **a** and **b** would undergo a S-S bond cleaving reaction with Ni-PF to give intermediate thiol, following by an intramolecular cyclization to generate the product **c**. To gain mechanistic insight into the reaction, several control experiments were conducted. When all of the optimized reaction conditions were eliminated, there was no product detected, which illustrated that the reaction could not proceed in the absence of the optimized reaction conditions (Supplementary Table 1). To study whether the reaction was proceeded via radical or ionic pathways, we performed a radical inhibition study using 2, 2, 6, 6-tetramethyl-1-piperidinyloxy (TEMPO) as a radical inhibitor. Two equivalents of TEMPO were added into the reaction to probe the radical nature of the reaction, and no corresponding **1c** was detected, indicating that the formation might be a free radical mediated reaction. While the adduct can be observed by high-resolution mass spectra (HRMS) in the reaction, suggesting that radicals are involved in the reaction (Figure S19). Besides, 2-aminobenzenethiol was subjected with **1b** to the optimized reaction conditions as a substitute of the toxic adduct, and successfully obtained the product **1c**. Thus, it was speculated that the product formation reaction was associated with the generation of radical intermediates.

Table 2. Substrate scope of symmetric disulfides by Ni-PF.[a,b]

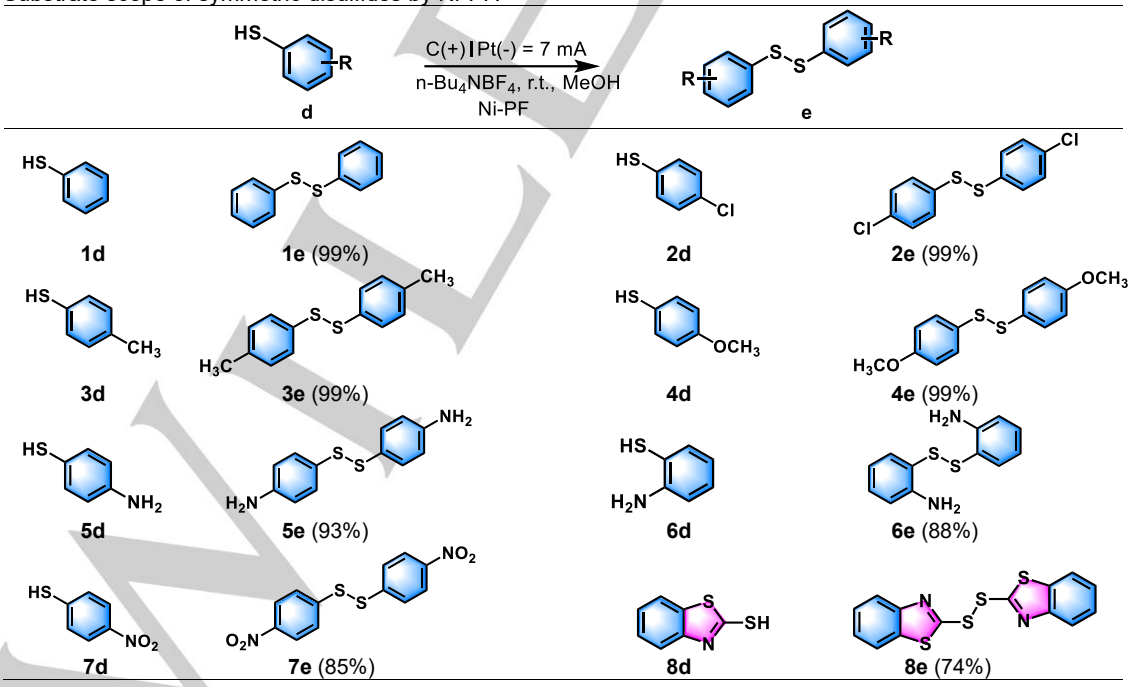

[a]Reaction conditions: carbon plate (53 mm * 8 mm * 1.5 mm) as anode, platinum plate (53 mm * 8 mm * 1.5 mm) as cathode, constant current (7 mA), d (0.2 mmol), Ni-PF (30 mg), n-Bu_4NBF_4 (0.25 mmol), CH_3OH (6 mL), r.t., 8 h. [b]Isolated yield.

10.1002/anie.202417439

Additionally, the electron density difference analysis was performed to study the interaction between the substrate and electrocatalyst, in which the red and blue electron clouds indicate electron aggregation and consumption, respectively (Figure 4a-c). We select 2,2'-disulfanediyldianiline (**1a**) as the model substrate to be interacted with M-PF (M = Ni, Cu and Zn). The electron density difference in electron distribution will display the charge transfer between the substrate and electrocatalyst to reflect the related interaction.[19] It can be seen that the electrons aggregate at the position of M-porphyrin center (M = Ni, Cu and Zn) and S site of 2,2'-disulfanediyldianiline (Figure 4a-c). Obviously, Ni-PF displays more obvious red electron density in interaction with 2,2'-disulfanediyldianiline when compared with Cu-PF and Zn-PF, implying Ni-PF has better interaction with the substrate. According to the above experimental results, a plausible reaction mechanism for the formation of 2-phenylbenzothiazole electrocatalyzed by Ni-PF is proposed in Figure 4d.[17b,18d,18e] Initially, the substrate is adsorbed on the catalyst, and then the substrate gets electrons to break its S-S bond to generate 2-mercaptonoaniline and sulfur radical intermediate. Furthermore, the amino group of sulfur radical intermediate and aldehyde group of benzaldehyde undergo aldimine condensation reaction to form intermediate. After that, sulfur radicals of intermediate attack the carbon atoms to realize the cyclization process. Finally, dehydration is carried out and the product is desorbed from the catalyst to complete the catalytic process (Figure 4d).

Density functional theory (DFT) calculations were further applied to elucidate the above proposed electrocatalytic mechanism and all geometries were fully optimized (Figure S20). Initially, we have calculated the free energy change (△G) of the systems under both U = 0 V and U = 5 V, and find that the energy barriers of the reaction steps are much lower under U = 5 V, indicating the electrocatalytic nature of the reaction catalyzed by M-PF (M = Ni, Cu and Zn) (Figure 4e and S21). Thus, we evaluate the mechanism based on the condition under U = 5 V. The adsorption steps of Ni-PF and Cu-PF are both exothermic ones with the values of -0.39 eV and -0.42 eV, respectively, while Zn-PF has the adsorption value of 0.00 eV, demonstrating that Ni-PF has better adsorption ability for the substrates (Figure 4e). Moreover, the aldimine condensation is the rate-determining step in the formation process of 2-phenylbenzothiazole. Considering that the energy barrier of rate-determining step for Ni-PF (-4.33 eV) is much lower than that of Cu-PF (-4.29 eV) and Zn-PF (-3.89 eV), the detected calculation results comply well with the experimental results (Figure 4e). Overall, triggered by electricity, Ni-PF with abundant active sites can serve as heterogenous redox mediator to interact with substrate. The substrate gets electrons subsequently to broke its S-S bond coupling with the generation of 2-mercaptonoaniline and sulfur radical intermediate. Then, the reaction undergoes aldimine condensation, cyclization and desorption processes to complete the catalytic process. During these processes, the functional Ni-PF with high robustness, durability and processability can tolerate the reaction processes to achieve high performance, holding much promise in potential flowing bed reactions or industrial-scale production. Besides, we have examined the intermediates of Ni-porphyrin with different spin multiplicities. We found that the spin density of Ni-porphyrin in both singlet and triplet states did not change during the catalytic processes (Figure S22 and S23).

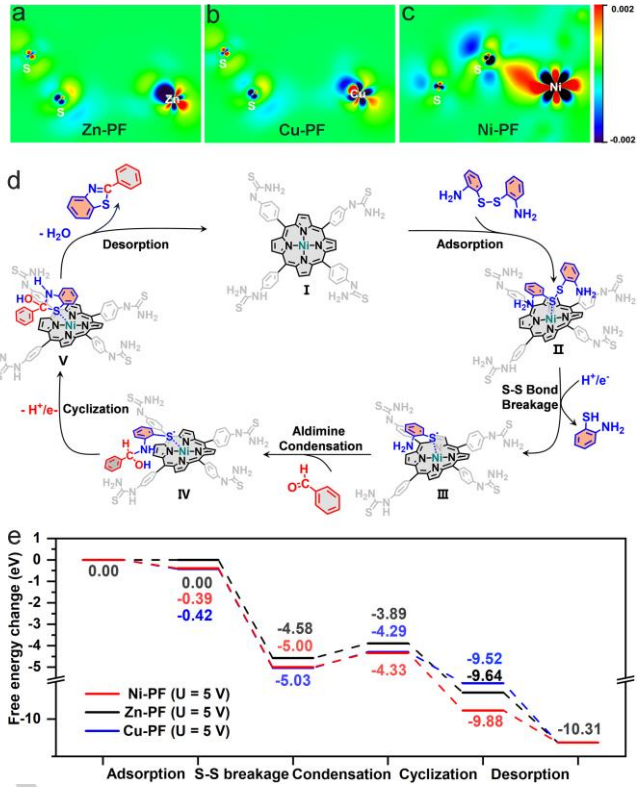

Figure 4. DFT calculations of M-PF (M = Ni, Cu and Zn). (a) Electron density difference before and after substrate adsorption of Zn-PF. (b) Electron density difference before and after substrate adsorption of Cu-PF. (c) Electron density difference before and after substrate adsorption of Ni-PF. (d) The plausible mechanism for the formation of 2-phenylbenzothiazole electrocatalyzed by Ni-PF. (e) Free energy change diagram of 2-phenylbenzothiazole formation under U = 5 V.

Conclusion

In summary, a series of metalloporphyrin-based polymer fibers (M-PF, M = Ni, Cu and Zn) have been reported through a rigid-flexible polymerization strategy based on rigid metalloporphyrin and flexible thiourea units. Specifically, the fabricated functional M-PF (M = Ni, Cu and Zn) with high strength and flexibility exhibit excellent interweavable and designable functions that can be readily processed into different fiber forms like knotted, two-spiral, three-ply, five-ply fibers or even interweaved networks. Interestingly, they can be readily applied in indirect electrocatalysis of benzothiazoles in S-S bond cleaving/cyclization reaction or extended oxidative self-coupling reaction of thiols with high efficiency. They can be easily recycled and enable to be fitted into gram-scale indirect electrocatalysis, which might promote the development of electrocatalysts with advanced processing forms.

Acknowledgements

This work was financially supported by the National Key R&D Program of China (2023YFA1507204). National Natural Science Foundation of China (Grants 22171139, 22225109, 22071109). Natural Science Foundation of Guangdong Province (No. 2023B1515020076).

Author contributions

Y.-Q. L., Y. C. and X. Y. conceived the idea. X. Y. and G. Y. designed the experiments, collected and analyzed the data. G. L., Y. H., C. H., Z. X., X. C, M. S., Y. Y. and X. H. assisted with the experiments and characterizations. X. Y. wrote the manuscript. All authors have approved the final version of the manuscript. # X. Y., G. L and Y. H. contributed equally to this work.

Competing interests

The authors declare no competing financial interests.

Keywords: Fiber catalyst, Indirect electrocatalysis, Redox mediator, Metalloporphyrin, Interweavable function

References

[1] A. Wiebe, T. Gieshoff, S. Möhle, E. Rodrigo, M. Zirbes, S. R. Waldvogel, *Angew. Chem. Int. Edit.* **2018**, *57*, 5594-5619.

[2] A. Shatskiy, H. Lundberg, M. D. Kärkäs, *ChemElectroChem* **2019**, *6*, 4067-4092.

[3] a) C. Ma, P. Fang, Z.-R. Liu, S.-S. Xu, K. Xu, X. Cheng, A. Lei, H.-C. Xu, C. Zeng, T.-S. Mei, *Sci. Bull.* **2021**, *66*, 2412-2429; b) R. Francke, R. D. Little, *Chem. Soc. Rev.* **2014**, *43*, 2492-2521; c) P. Chakraborty, R. Mandal, N. Garg, B. Sundararaju, *Coordin. Chem. Rev.* **2021**, *444*, 214065.

[4] a) C. Zhu, N. W. J. Ang, T. H. Meyer, Y. Qiu, L. Ackermann, *ACS Central Sci.* **2021**, *7*, 415-431; b) K. Mitsudo, *Chem. Rec.* **2021**, *21*, 2269-2276; c) Z. N. Gafurov, A. O. Kantyukov, A. A. Kagilev, O. G. Sinyashin, D. G. Yakhvarov, *Coordin. Chem. Rev.* **2021**, *442*, 213986.

[5] H. Fei, J. Dong, D. Chen, T. Hu, X. Duan, I. Shakir, Y. Huang, X. Duan, *Chem. Soc. Rev.* **2019**, *48*, 5207-5241.

[6] a) Z. Weng, J. Jiang, Y. Wu, Z. Wu, X. Guo, K. L. Materna, W. Liu, V. S. Batista, G. W. Brudvig, H. Wang, *J. Am. Chem. Soc.* **2016**, *138*, 8076-8079; b) M. Arif, M. Babar, U. Azhar, M. Sagir, M. Bilal Tahir, M. Asim Mushtaq, G. Yasin, M. Mubashir, J. Wei Roy Chong, K. Shiong Khoo, P. Loke Show, *Chem. Eng. J.* **2023**, *451*, 138320; c) K. Yamamoto, M. Kuriyama, O. Onomura, *Acc. Chem. Res.* **2020**, *53*, 105-120.

[7] G. Liu, Y. Chen, Y. Chen, Y. Shi, M. Zhang, G. Shen, P. Qi, J. Li, D. Ma, F. Yu, X. Huang, *Adv. Mater.* **2023**, *35*, 2304716.

[8] a) F. Sun, H. Jiang, H. Wang, Y. Zhong, Y. Xu, Y. Xing, M. Yu, L.-W. Feng, Z. Tang, J. Liu, H. Sun, H. Wang, G. Wang, M. Zhu, *Chem. Rev.* **2023**, *123*, 4693-4763; b) T. Xu, Z. Zhang, L. Qu, *Adv. Mater.* **2020**, *32*, 1901979; c) Z. Dong, C. Jiang, H. Cheng, Y. Zhao, G. Shi, L. Jiang, L. Qu, *Adv. Mater.* **2012**, *24*, 1856-1861; d) Y. Dou, Z.-P. Wang, W. He, T. Jia, Z. Liu, P. Sun, K. Wen, E. Gao, X. Zhou, X. Hu, J. Li, S. Fang, D. Qian, Z. Liu, *Nat. Commun.* **2019**, *10*, 5293; e) X. Leng, X. Zhou, J. Liu, Y. Xiao, J. Sun, Y. Li, Z. Liu, *Mater. Horiz.* **2021**, *8*, 1538-1546; f) C. Z. Liang, M. Askari, L. T. Choong, T.-S. Chung, *Nat. Commun.* **2021**, *12*, 2338.

[9] Q. Shi, J. Sun, C. Hou, Y. Li, Q. Zhang, H. Wang, *Adv. Fiber Mater.* **2019**, *1*, 3-31.

[10] a) Z. Gao, J. Zhu, S. Rajabpour, K. Joshi, M. Kowalik, B. Croom, Y. Schwab, L. Zhang, C. Bumgardner, K. R. Brown, D. Burden, J. W. Klett, A. C. T. van Duin, L. V. Zhigilei, X. Li, *Sci. Adv.* **2020**, *6*, eaaz4191; b) F. Zhang, J. Chen, J. Yang, *Adv. Fiber Mater.* **2022**, *4*, 720-735; c) L. Wang, F. Zhang, Y. Liu, J. Leng, *Adv. Fiber Mater.* **2022**, *4*, 5-23; d) J. Feng, H. Peng, *Chinese J. Chem.* **2022**, *40*, 1705-1713; e) Z. Qiao, C. Ding, *Ionics* **2022**, *28*, 5259-5273; f) Y. Meng, Y. Zhao, C. Hu, H. Cheng, Y. Hu, Z. Zhang, G. Shi, L. Qu, *Adv. Mater.* **2013**, 25, 2326-2331.

[11] a) Y. Wen, M. Jian, J. Huang, J. Luo, L. Qian, J. Zhang, *Nano Lett.* **2022**, 22, 6035-6047; b) H. Li, R. Qu, Z. Ma, N. Zhou, Q. Huang, Z. Zheng, *Adv. Funct. Mater.* **2023**, *n/a*, 2308120; c) Z. Kong, Y. Hou, J. Gu, F. Li, Y. Zhu, X. Ji, H. Wu, J. Liang, *Nano Lett.* **2023**, *23*, 6216-6225; d) J. Sun, H. He, K. Zhao, W. Cheng, Y. Li, P. Zhang, S. Wan, Y. Liu, M. Wang, M. Li, Z. Wei, B. Li, Y. Zhang, C. Li, Y. Sun, J. Shen, J. Li, F. Wang, C. Ma, Y. Tian, J. Su, D. Chen, C. Fan, H. Zhang, K. Liu, *Nat. Commun.* **2023**, *14*, 5348; e) Y. Bai, R. Zhang, X. Ye, Z. Zhu, H. Xie, B. Shen, D. Cai, B. Liu, C. Zhang, Z. Jia, S. Zhang, X. Li, F. Wei, *Nat. Nanotechnol.* **2018**, *13*, 589-595; f) C. Gleissner, J. Landsiedel, T. Bechtold, T. Pham, *Polym. Rev.* **2022**, *62*, 757-788.

[12] H. Pan, Z. Cheng, H. Zhong, R. Wang, X. Li, *ACS Appl. Mater. Interfaces* **2019**, *11*, 8032-8039.

[13] X. Yao, C. Guo, C. Song, M. Lu, Y. Zhang, J. Zhou, H.-M. Ding, Y. Chen, S.-L. Li, Y.-Q. Lan, *Adv. Mater.* **2023**, *35*, 2208846.

[14] Q.-J. Wu, D.-H. Si, Q. Wu, Y.-L. Dong, R. Cao, Y.-B. Huang, *Angew. Chem. Int. Edit.* **2023**, 62, e202215687.

[15] a) C. G. Mortimer, G. Wells, J.-P. Crochard, E. L. Stone, T. D. Bradshaw, M. F. G. Stevens, A. D. Westwell, *J. Med. Chem.* **2006**, *49*, 179-185; b) P. C. Sharma, A. Sinhmar, A. Sharma, H. Rajak, D. P. Pathak, *J. Enzym. Inhib. Med. Ch.* **2013**, *28*, 240-266; c) R. K. Gill, R. K. Rawal, J. Bariwal, *Arch. Pharm.* **2015**, *348*, 155-178; d) M. Al-Talib, Y. A. Al-Soud, M. Abussaud, S. Khshashneh, *Arab. J. Chem.* **2016**, *9*, S926-S930; e) H.-J. Cho, A. K. Sharma, Y. Zhang, M. L. Gross, L. M. Mirica, *ACS. Chem. Neurosci.* **2020**, *11*, 1471-1481.

[16] Q.-J. Wu, D.-H. Si, Q. Wu, Y.-L. Dong, R. Cao, Y.-B. Huang, *Angew. Chem. Int. Edit.* **2023**, 62, e202215687.

[17] a) Z. Liu, Z. Chen, H. Tong, M. Ji, W. Chu, *Green Chem.* **2023**, *25*, 5195-5205; b) Q. Lu, L. Zhao, L. Wu, X. Wang, G. Shen, X. Huang, M. Du, D. Ma, *ChemistrySelect* **2022**, *7*, e202104081; c) E. A. Jaseer, D. J. C. Prasad, A. Dandapat, G. Sekar, *Tetrahedron Lett.* **2010**, *51*, 5009-5012; d) Z. Li, C. Zhou, R. Ye, L.-G. Meng, *Green Chem.* **2022**, *24*, 3845-3849; e) J. Shi, D. Qiu, J. Wang, H. Xu, Y. Li, *J. Am. Chem. Soc.* **2015**, *137*, 5670-5673; f) X.-Y. Qian, S.-Q. Li, J. Song, H.-C. Xu, *ACS Catal.* **2017**, *7*, 2730-2734; g) D. Ma, S. Xie, P. Xue, X. Zhang, J. Dong, Y. Jiang, *Angew. Chem. Int. Edit.* **2009**, *48*, 4222-4225; h) K. Inamoto, C. Hasegawa, J. Kawasaki, K. Hiroya, T. Doi, *Adv. Synth. Catal.* **2010**, *352*, 2643-2655.

[18] a) Y.-F. Wang, M.-Y. Qi, M. Conte, Z.-R. Tang, Y.-J. Xu, *Angew. Chem. Int. Edit.* **2023**, *62*, e202304306; b) M. Y. S. Ibrahim, G. R. Cumming, R. Gonzalez de Vega, P. Garcia-Losada, O. de Frutos, C. O. Kappe, D. Cantillo, *J. Am. Chem. Soc.* **2023**, *145*, 17023-17028; c) M. Wang, C. Zhang, C. Ci, H. Jiang, P. H. Dixneuf, M. Zhang, *J. Am. Chem. Soc.* **2023**, *145*, 10967-10973; d) C. Guan, J. Yin, J. Ji, J. Liu, X. Wu, T. Zhu, S. Liu, *Org. Lett.* **2023**, *25*, 5383-5388; e) K. S. Bhati, D. Suwalka, V. P. Verma, A. K. Jassal, N. Kumari, S. Sharma, *Org. Lett.* **2023**, *25*, 5421-5425; fY. Lin, T. von Münchow, L. Ackermann, *ACS Catal.* **2023**, *13*, 9713-9723; g) M. Zhang, B.-B. Zhang, Q. Lin, Z. Jiang, J. Zhang, Y. Li, S. Pei, X. Han, H. Xiong, X. Liang, Y. Lin, Z. Wei, F. Zhang, X. Zhang, Z.-X. Wang, Q. Shi, H. Huang, *Angew. Chem. Int. Edit.* **2023**, *62*, e202306307.

[19] T.-Y. Yu, Q. Niu, Y. Chen, M. Lu, M. Zhang, J.-W. Shi, J. Liu, Y. Yan, S.-L. Li, Y.-Q. Lan, *J. Am. Chem. Soc.* **2023**, *145*, 8860-8870.

10.1002/anie.202417439

WILEY-VCH

RESEARCH ARTICLE

Entry for the Table of Contents

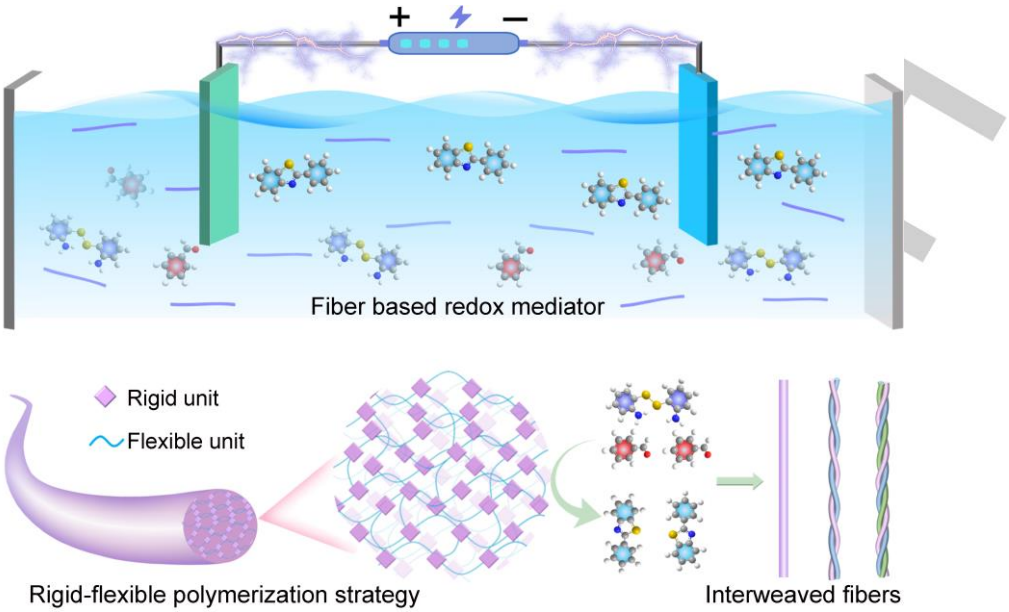

A series of mechanically robust metalloporphyrin-based polymer fibers were fabricated through the condensation of rigid metalloporphyrin and flexible thiourea units and exhibited high indirect electrocatalytic efficiency.